



Provided by the author(s) and University College Dublin Library in accordance with publisher policies. Please cite the published version when available.

Title	Effect of Road Surface, Vehicle, and Device Characteristics on Energy Harvesting from pÿ Bridge Vehicle Interactions
Authors(s)	Cahill, Paul; Jaksic, Vesna; Keane, John; Pakrashi, Vikram; et al.
Publication date	2016-08-22
Publication information	Computer-Aided Civil and Infrastructure Engineering, 31 (12): 921-935
Publisher	Wiley Online Library
Item record/more information	http://hdl.handle.net/10197/10443
Publisher's statement	This is the peer reviewed version of the following article: Cahill, P. , Jaksic, V. , Keane, J. , O'Sullivan, A. , Mathewson, A. , Ali, S. F. and Pakrashi, V. (2016), Effect of Road Surface, pÿ Vehicle , and Device Characteristics on Energy Harvesting from pÿ Interactions. Computer Aided Civil and Infrastructure Engineering. This article has been published in final form at http://onlinelibrary.wiley.com/doi/10.1111/mice.12228 . This article may be used for non-commercial purposes in accordance with Wiley Terms and Conditions for Self-Archiving.
Publisher's version (DOI)	10.1111/mice.12228

Downloaded 2020-06-10T12:34:17Z

The UCD community has made this article openly available. Please share how this access benefits you. Your story matters! (@ucd_oa)



Some rights reserved. For more information, please see the item record link above.



Effect of Road Surface, Vehicle and Device Characteristics on Energy Harvesting from Bridge-Vehicle Interactions

Paul Cahill

Beaufort/MaREI Research, Environmental Research Institute, University College Cork, Ireland and Dynamical Systems and Risk Laboratory, Civil, Structural and Environmental Engineering, University College Cork, Cork, Ireland

Vesna Jaksic

Beaufort/MaREI Research, Environmental Research Institute, University College Cork, Ireland and Dynamical Systems and Risk Laboratory, Civil, Structural and Environmental Engineering, University College Cork, Cork, Ireland

John Keane

Dynamical Systems and Risk Laboratory, Civil, Structural and Environmental Engineering, University College Cork, Cork, Ireland

Anthony O'Sullivan

Dynamical Systems and Risk Laboratory, Civil, Structural and Environmental Engineering, University College Cork, Cork, Ireland

Alan Mathewson

Heterogeneous Systems Integration Group, Microsystems Group, Tyndall National Institute, University College Cork, Ireland

Shaikh Faruque Ali

Department of Applied Mechanics, Indian Institute of Technology – Madras, India

&

Vikram Pakrashi*

Dynamical Systems and Risk Laboratory, Civil, Structural and Environmental Engineering, University College Cork, Cork, Ireland

Abstract: *Energy harvesting for powering sensors for structural health monitoring has received huge attention worldwide. A number of practical aspects affecting energy harvesting and leading to the possibility of health monitoring directly from energy harvesters is investigated here. The key idea is the amount of power received from a damaged and an undamaged structure vary and the signature of such variation can be used for Structural Health Monitoring (SHM). For this study, a damaged and an undamaged bridge are considered with harvesters located at different positions and the power harvested is accessed numerically as to how energy harvesting can act as a damage detector and monitor. Bridge-vehicle interaction is exploited to harvest energy. For a damaged bridge, a bilinear breathing crack is considered. Variable surface roughness according to ISO 8606:1995(E) is considered such that the real values can be considered in*

the simulation. The possibility of a drive-by type health monitoring using energy harvesting is highlighted and the effects of road surface on such monitoring are identified. The sensitivity of the harvester health monitoring to locations and extents of crack damage are reported. The effects of multiple harvesters harvested power are discussed along with effects of vehicular parameters. Continuous harvesting over a length of the bridge is considered semi-analytically. A comparison among the numerical simulations, detailed Finite Element analysis and experimental results emphasizes the feasibility of the proposed method.

1 INTRODUCTION

Self-powered sensors can have a significant impact on the structural health monitoring (SHM) of bridges as they can survive on small quantities of energy harvested from

ambient sources (Sodano et al., 2004). Sensing based on miniaturized, reliable and almost maintenance-free sensor nodes is thus increasingly attractive due to the prospect of low maintenance and easy data-collection and transfer of data to a centralized repository. In cases of large infrastructures such as bridges, dams and buildings, these sensors can have a distinct advantage over traditional battery-driven sensors due to their self-powered nature (Beeby et al., 2006).

One of the potential applications of energy harvesting lies in the operation of highway bridges. Unhindered use of highway bridges is vital for local, national and international transportation networks. An interruption in their operation during inspection, maintenance or repair can result in expensive delays and affect the economic and social wellbeing of a society (Pakrashi et al., 2011). A Structural Health Monitoring (SHM) system can therefore be important to maximise efficiency and costs associated with long term monitoring of bridge infrastructure so as not to hinder economic activities and safety. One such system that has the potential to achieve this is the use of a Wireless Sensor Network (WSN) coupled with energy harvesting technology (Fu et al., 2013, Cho and Spencer, 2015).

Monitoring of large scale civil structures using WSN's has been established in recent years but is yet to become widespread (Lynch, 2007). Full scale monitoring of highway bridges (Kim et al., 2007) and pedestrian bridges being accomplished (Rice et al., 2010) and such investigations can provide real-time monitoring (Torbol, 2014) of the structures, which is particularly important for the detection of growth of existing cracks and development of fresh cracks in fracture prone bridges (Fasl et al., 2011). The cost and minimal disruption during installation of a WSN makes it an attractive alternative to traditional wired SHM systems (Lynch and Loh, 2006; Park et al., 2010). A difficulty faced with the successful deployment of WSN's relate to the availability of adequate power sources for individual sensor nodes of the network. Battery replacement can prove to be both disruptive and expensive (Erturk, 2011). This negates many of the advantages associated with damage detection using WSN's and creates an opportunity to investigate new solutions.

The use of energy harvesting technology to support WSN's has received increased attention in recent times, with solar, wind and vibration based energy harvesting being investigated (Lynch, 2007; Elvin et al., 2006). There has been significant research into the development of energy harvesting devices utilising ambient vibration (Beeby et al., 2006), which is particularly suitable for civil infrastructure. This allows for applications including powering of small scale electronic devices (Arms et al., 2005), structural health monitoring (Kaur and Bhalla, 2014), wireless health monitoring (Farinholt et al., 2010) and semi-active control (Shen et al., 2011). The primary vibration based energy harvesters being investigated are

piezoelectric (Ali et al., 2010), electro-magnetic (Mann and Sims, 2009), coupled piezo-electromagnetic (Challa et al., 2009) or piezo-magnetoelastic (Ali et al., 2011a).

There have been recent studies on vibration based energy harvesting from bridge infrastructure, with bridge – vehicle interaction being considered for both highway bridges (Ali et al., 2011a; Sazonov et al., 2009, Keane et al., 2012) and railway bridges (Cahill et al., 2014). These studies indicate the possibility of using energy harvesting from bridges due to vehicular passage for monitoring purposes and also highlights the importance of understanding the effects various factors have in terms of understanding, assessing and interpreting the variations in energy harvesting. Utilizing bridge – vehicle interaction ensures that the energy is generated under operational conditions and while research into energy harvesting from this interaction is in its infancy, the modelling of the interaction is quite well established (Fryba, 1999; Green and Cebon, 1994; Gillespie et al., 1993; Abdel-Rohman and Al-Duaij, 1996; Delgado and dos Santos, 1997; Pakrashi et al., 2010a; Pesterev and Bergman, 1997; Song et al., 2003; Andersson, 2015). In this regard, a comparison of the effects of various parameters on such energy harvesting, in combination with benchmarks related to detailed modelling and experimental results can lead to the advancement of the potential use of energy harvesting as a practical SHM tool. This paper quantitatively assesses the effects of some key operational parameters in terms of energy harvesting from bridge-vehicle interactions. The analytical model is compared against a detailed Finite Element model and experimental results. They include damage effects in the form of a breathing crack, broadband interaction of the vehicle with the surface roughness of the bridge, effects of vehicle mass and stiffness, tuning of the harvester and vehicle speed. The use of multiple harvesters, the effect of multiple vehicles and continuous harvesting have also been discussed. The study is expected to be of importance in guiding practical decisions behind energy harvesting from bridge-vehicle interaction and the choice of applications of such harvesting without having to carry out detailed experimental investigations.

2MODELLNG OF DAMAGED BRIDGE – VEHICLE INTERACTION AND A PIEZOELECTRIC ENERGY HARVESTER

When attached to the host structure, piezoelectric energy harvesters can utilise the dynamic acceleration response due to damaged bridge – vehicle interaction to generate energy. The acceleration responses act as base excitation for the harvesters, resulting in energy being generated. The amount of energy which can be harvested from the system is dependent on both the dynamic response of the bridge due to the passage of the vehicle and the properties of the energy harvester. The maximum energy harvested can be

linked to the tuning of the harvester and the optimization of the circuit that is used to store the energy. In this paper, optimization of circuitry is not the main focus and consequently as standard circuit comprising of a simple resistance is considered. This is adequate when using harvested energy for monitoring purposes.

To observe the variation of energy harvested due to the full interaction of surface roughness, dynamic coupling of the vehicular degree of freedom and the effect of damage, a model is developed (Figure 1) for simulation based on first principles and resulting set of differential equations. Such equations are not difficult to solve numerically and can be excellent for carrying out detailed studies replacing computationally intensive Finite Element models.

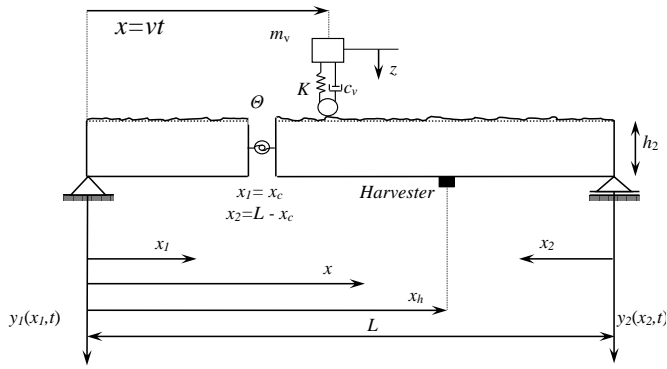


Figure 1. Analytical model of a damaged bridge with attached piezoelectric energy harvester being traversed by a vehicle.

2.1 Modelling of Damaged Bridge–Vehicle Interaction

A simply supported Euler – Bernoulli beam with a bilinear breathing crack traversed by a single degree of freedom (SDOF) oscillator (Figure 1) is considered. The beam, of length L , has a crack at a distance x_c from the left support and has a constant cross-sectional area A and second moment of area I respectively. Considering $y_i(x, t)$ as the transverse deflection of the i^{th} beam at a location of distance x from the left support and time t , measured from the static equilibrium position, the equation of motion of the interaction between the bridge and the moving oscillator is given by (Fryba, 1999).

$$EI \frac{\partial^4 y_i(x, t)}{\partial x^4} + c \frac{\partial y_i(x, t)}{\partial t} + \rho A \frac{\partial^2 y_i(x, t)}{\partial t^2} = \bar{P} \delta(x - vt)$$

$$i = 1, 2 \quad (1)$$

$$y_i(x_i, t) = \sum_{i=1}^n \phi_i(x_i) q_i(t) \quad (2)$$

Where EI is the flexural rigidity, E is the Young's modulus of the material of the beam, c is the structural

damping of the beam, ρA is the mass per unit length, ρ is the mass per unit volume of the beam, δ is the Dirac Delta function and vt is the position of the vehicle from left support, where v is the constant speed of the vehicle. The transverse deflection is given by Equation 2, where $\phi(x)$ is the mode shape and $q(t)$ is the time dependent amplitude.

The force \bar{P} , caused by the moving vehicle, modelled as a moving oscillator, is defined as (Schenk and Bergman, 2003).

$$\bar{P} = \{m_v g - c_v [\dot{z} - \dot{y}_i(vt, t) - \dot{r}(vt)] - K[z - y_i(vt, t) - r(vt)]\}$$

$$i = 1, 2 \quad (3)$$

Where m_v is the mass of the vehicle, g is acceleration due to gravity, c_v is vehicle damping coefficient, K is the stiffness of the vehicle's tires and springs and z is the vertical displacement of the vehicle with respect to its static equilibrium position. The surface roughness is given by r and an overdot indicates differentiation with respect to time. For solutions involving cases with an undamaged bridge, it is representative of a closed crack. The bridge is therefore modelled as a continuous beam. The natural frequencies, ω_n , and the modeshapes are reduced to those obtained for a standard simply supporting Euler – Bernoulli beam, given by

$$\omega_n = \sqrt{\frac{\lambda^4 EI}{\rho A}} \quad (4)$$

where λ is a constant dependent on the beam model characteristics. Consideration of only the first mode shape is sufficiently accurate in representing the dynamic response of the undamaged bridge model for a significant majority of cases (Yang and Lin, 2005; Pakrashi et al., 2010b). While higher modes can participate in energy harvesting, the effect of the first bending mode will still govern for a large number of cases, especially for road bridges and when the harvesters are installed to capture vibration principally in that direction. Therefore when considering the undamaged beam model, only the first mode shape is utilised in this paper.

The crack is represented as an open crack and the system consists of two beams being connected by means of a spring-mass system being in torsion. Each continuous segment of the beam can be described by the Euler–Bernoulli partial differential equation of motion (Narkis, 1994; Sundermeyer and Weaver, 1994; Jaksic et al., 2014). The slope between the two beam segments can be related to the moment at this section through the assumption of an equivalent rotational spring at the location of damage. Kinematic boundary conditions related to the displacements and slopes at the boundaries are retained. The displacement compatibility and shear transfer are also assumed at the location of damage, while the integral of the square of modeshape is normalized to unity. The dynamic response of the bridge and the vehicle are obtained through the

conversion of the Dirac Delta function of the spatial variable into the time domain and subsequent use of the Runge-Kutta Methods to solve the coupled second order ODEs.

2.2 Modelling of Road Surface Roughness

Road Surface Roughness (RSR), r , can be represented by a periodic modulated random process (Wu and Law, 2011). In ISO 8606:1995(E) specifications, RSR is related to the speed of the vehicle through velocity and displacement power spectral densities (PSDs), where the general form of displacement PSD of RSR is

$$S_d(f) = S_d(f_0) \left(\frac{f}{f_0} \right)^{-\alpha} \quad (5)$$

where $f_0 = 1/2\pi$ is the discontinuity frequency, f is the spatial frequency, $S_d(f_0)$ is roughness coefficient and α is an exponent of the PSD. In this paper, this roughness classification is based on constant vehicle velocity and $\alpha = 2$. The RSR function $r(\hat{x})$ in time domain can be simulated by applying the inverse Fourier transformation on $S_d(f_0)$ given as (Henchi et al., 1998).

$$r(\hat{x}) = \sum_{k=1}^N \sqrt{4S_d(f_0) \left(\frac{2\pi k}{\tilde{L}_c f_0} \right)^{-2}} \frac{2\pi}{\tilde{L}_c} \cos \left(\frac{2\pi k f_0}{\tilde{L}_c} \hat{x} + \theta_k \right) \quad (6)$$

where \tilde{L}_c is twice the length of the bridge, N is the number of data points of successive ordinates of surface profile and θ_k is a set of independent random phase angles uniformly distributed between 0 and 2π . This paper considers the case of five different classes of road surface roughness conditions, ranging from very good to very poor (Table 1) and Figure 2 presents examples of these road conditions.

Table 1. Surface Roughness Conditions based on ISO 8606:1995(E).

Road Class	A Very Good	B Good	C Average	D Poor	E Very Poor
Roughness Coefficient $S_d(f_0)(m^3/cycle) \times 10^{-6}$	6	16	64	256	1024

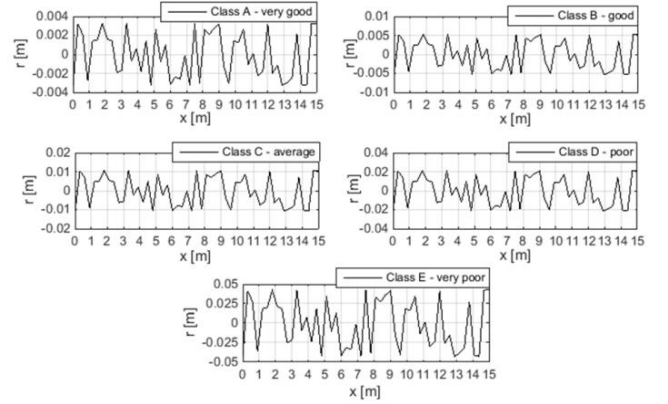


Figure 2. The example of the road Surface Roughness Conditions for Five Classes calculated according to ISO 8606:1995(E).

2.3 Modelling of Piezoelectric Energy Harvester

Cantilever piezoelectric energy harvesters are considered in this paper. The electrical circuit does not have any inductor due to the very low excitation frequencies from the host structure. The inclusion of an inductor circuit would lead to a high optimum value for inductance. This would consume power and lead to lower outputs. Vibration based piezoelectric harvesters are designed with and without inductor in the circuit. The electrical parameters of designed harvester are optimized to generate high power at a particular frequency. These parameters are electrical resistance, electro-mechanical coupling factor and electrical time constants and inductance (for harvesters with inductor). Optimal values of inductance are either zero or frequency dependent (Renno et al., 2009). For low frequencies the inductance values comes out to be quite high and this needs large inductors, which in turn increases the size of the harvester. Therefore, in the analysis it is considered that the inductance value is zero. The cantilever harvester with a tip mass has piezoelectric materials bonded to its upper and lower surfaces using a base substrate (Figure 3). The piezoelectric materials are between two electrode layers which carry the generated charge from the material whilst undergoing excitation. The electromechanical behaviour of the energy harvester is represented by the coupled linear ordinary differential equations (ODEs) as in (Ali et al., 2011b)

$$m_h \ddot{z}_h + c_h \dot{z}_h + k_h z_h - \theta V = -m_h \ddot{y}(x, t) \quad (7)$$

$$\theta \dot{z}_h + C_p \dot{V} + \frac{1}{R_l} V = 0 \quad (8)$$

where $z_h(t)$ is the relative dynamic displacement of the mass of the harvester, m_h , the equivalent viscous damping is given as c_h and k_h is the stiffness of the harvester. The electromechanical coupling of the harvester is given by θ , C_p and $V(t)$ are the capacitance and voltage across the

piezoelectric material, respectively, while R_l is the resistance across the load resistor. The base excitation which is applied to the harvester, $\ddot{y}(x_h, t)$, is obtained from the acceleration of the bridge at the location at which the harvester is located. The mechanical coupling between the harvester and bridge is disregarded as harvester has a significantly lower mass as compared to the bridge and it will have negligible impact on the bridge dynamics. The total harvested energy, E_h , obtained from the energy harvester can be determined through the integration of the instantaneous power, giving

$$E_h = \int_0^{\bar{T}} \frac{V(t)^2}{R_l} dt \quad (9)$$

where \bar{T} is the time taken by the vehicle to cross the bridge. Theoretically, even after the passage of the vehicle over the bridge ambient vibration remains and energy may be harvested at a very low level. Such levels are difficult to utilise for monitoring due to their value and presence of high noise, and are not considered in this paper.

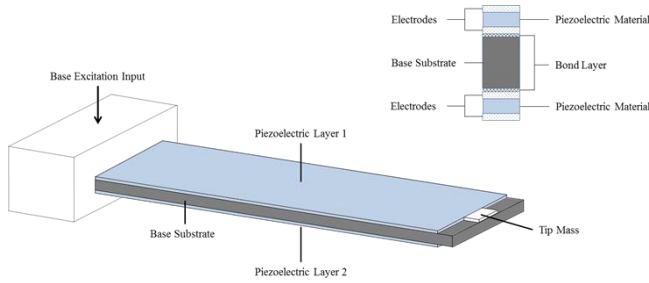


Figure 3. Schematic of piezoelectric energy harvester with general arrangement and cross section.

2.4 Parameters for Energy Harvesting From Bridge – Vehicle Interaction

The static deflection of the bridge was set to $0.005m$ for a static point load at the centre of a simply supported structure due to a vehicle of weight $3000kg$ and it was assumed that the depth of the bridge is 1.5 times the depth of the beam, so that the second moment of area of the cross-section remains unaltered. From this, other geometric descriptors can be computed; such the second moment of area about the neutral axis I , and the equivalent quantities that give rise to this deflection. These numbers have been previously used by Jaksic et al. (2014) for introducing a new technique for structural health monitoring using bridge-vehicle interaction and the use of these numerical values link the current study to the benchmark of responses already established through Jaksic et al. (2014). To maximise the amount of energy which can be harvested from bridge – vehicle interaction, the harvester is tuned to the natural frequency of the bridge and its optimal parameters subsequently determined (Ali et al., 2011a; Ali

et al., 2011b). The parameters of the bridge, those used for vehicle simulation (Law and Zhu, 2004) and the general parametric values for the energy harvester (Ali et al., 2011b; Elvin et al., 2006) are provided in Table 2. For the energy harvester, α is the non-dimensional time constant of the first-order electrical system non-dimensionalized and given by $\alpha = \omega_h C_p R_l$, with ω_h being the natural frequency of the mechanical system.

Table 2. Bridge, vehicle and energy harvester parameters used in simulation

	Symbol	Value	Unit
Bridge			
Length	L	15	m
Damping ratio	ζ	2	%
Youngs Modulus	E	200 x 10^9	N/m ²
Density	P	7900	Kg/m ³
Second moment of area about the neutral axis	I	0.0021	m ⁴
Height	h	0.439	m
Breadth	b	0.293	m
Cross-Sectional Area	A	0.1287	m ²
Vehicle			
Mass	m_v	3000	kg
Damping	c_v	3.0159 x 10^3	N-s/m
Stiffness	K	3.65 x 10^6	N/m
Harvester			
Tip Mass	m_h	2.5	g
Equivalent Viscous Damping Ratio	γ_h	0.038	
Stiffness	k_h	0.4286	N/m
Natural Frequency	ω_h	2.084	Hz
Electromechanical Coupling	θ	7.501	$\mu C/m$
Capacitance of the Piezoceramic	C_p	2.866	nF
Non-dimensional Time Constant	α	0.9	

A typical example of the dynamic response mid-span of the model bridge is illustrated which is also the location of the harvester on this occasion, with a Crack Depth Ratio (CDR) of 0.05 at the centre of the beam and considering poor surface roughness conditions for a vehicular passage at 80 km/hr (Figure 2). The displacement (Figure 4a), velocity (Figure 4b), acceleration (Figure 4c) and phase space (Figure 4d) are illustrated. Following from this dynamic response of the beam, the amount of energy harvested during such a passage proved to be of the order of $1.53\mu J$.

For the purposes of creating a baseline model a set of parameters were chosen (Table 2) and the values of different parameters are changed with respect to this baseline model in this paper. The energy harvesting potential from an undamaged bridge with RSR Class A, *i.e.*, very good road surface, for a range of vehicle speeds was determined and shown in Figure 5. As can be seen, there exists a bandwidth for the vehicle speed at which harvester scavenges the maximum amount of energy, between 8 and

12m/s. The peak value of harvested energy lies within this region, with a total of $0.02\mu J$ of energy obtained for a vehicle speed of 8m/s, while vehicle speeds outside of this bandwidth generate notably lower levels of energy. Considering the optimal vehicle speeds for energy harvesting, the range depends on the bridge-vehicle interaction parameters and is unique for a combination of parameters.

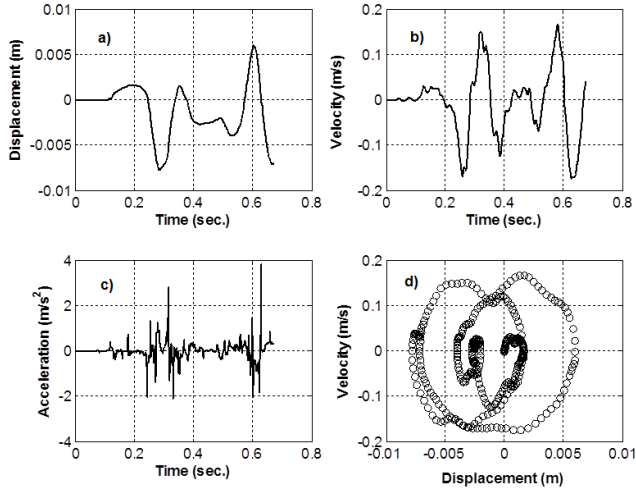


Figure 4. Output dynamic response of the Bridge-Vehicle Interaction model. The vehicle speed is 80km/hr and a CDR at the centre is considered to be 0.005. The harvester is located at mid-span.

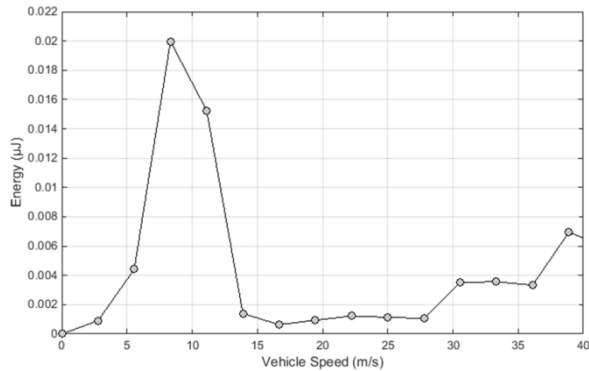


Figure 5. Energy harvested from passage of vehicle at varying speeds along undamaged model with very good RSR conditions. The harvester is located at mid-span.

3IMPACT OF BRIDGE AND ROAD CONDITIONS ON ENERGY HARVESTING

This section simulates the effect of damage in bridge and road surface condition on the harvested energy.

3.1 Energy Harvesting from Damaged Bridge – Vehicle Interaction

Varying effects of damage on the bridge model were considered for the study. The RSR is fixed at Road Class E, *i.e.*, Very Poor. The breathing crack, as represented by the spring, was positioned at three locations along the bridge (mid-span, quarter-span and 1m from support) with varying magnitude. At each of the chosen damage locations, three different magnitudes of damage were investigated, ranging from small (CDR=0.05), medium (CDR=0.2) to large (CDR=0.35). For every damage case, a range of vehicle speeds are considered, to a maximum of 40 m/s. The energy harvesting potential for each case is determined and reported.

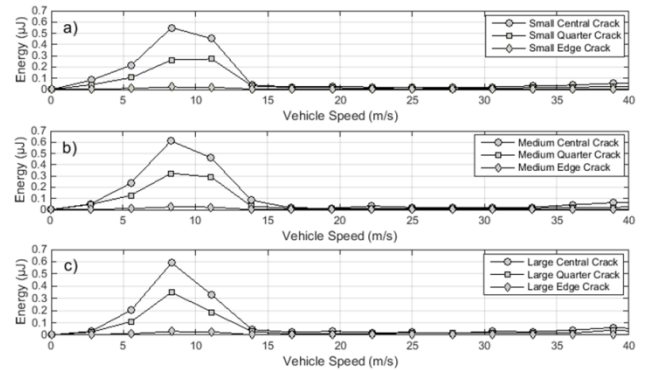


Figure 6. Effect of variation in location and magnitude of damage on energy harvested for a) small, b) medium and c) large crack when harvester is positioned at half span. Maximum power is generated with vehicle velocities between 8m/s to 12m/s.

For the range of vehicle speeds and a harvester at mid-span, it was found that an optimum range for energy harvesting exists between 8 and 12m/s, which is consistent with the undamaged case (Figure 6) when harvester the positioned at mid-span. For all cases of damage considered, the peak energy harvester outputs were found within this bandwidth, with the levels of energy harvested ranging from $0.05\mu J$ to $0.6\mu J$. Compared with the baseline case; this represents an order of magnitude increase in the energy harvesting output with increasing damage. The influence of a central crack was found to have the biggest effects on the energy harvesting, as expected, with all three levels of CDR providing a greater magnitude in output than the quarter crack. The quarter crack in turn was greater than the edge crack, which produced only minor differences in energy harvesting output when compared to the baseline model. At the optimal vehicle speed for energy harvesting, 8m/s, the medium crack provides a bigger magnitude for all three locations of damage than its large crack counterpart. This

difference in magnitude is however relatively small and as a whole, the actual degree of damage provides only minor variations in the energy harvesting outputs at each location considered. It is therefore the actual location of the damage along the bridge which causes the greatest influence on energy harvesting outputs as opposed to the magnitude of the damage. Once the location is established, small changes focused at that specific location, will be indicative of the extent of damage.

3.2 Effects of Road Surface Conditions on Energy Harvesting

The conditions of a road surface affect the dynamic response of a bridge under vehicular loading (O'Brien et al., 2006; Jaksic et al., 2011; Jaksic et al., 2012) and will in turn influence the quantity of energy that can be harvested. The condition of a road can vary significantly, depending on its age, location and funding available for refurbishment. Therefore it is an important parameter when considering the effects of bridge degradation on energy harvesting potential. In this investigation, a 3T load, a central crack location with CDR=0.1 are considered, with the effects of five different classes of RSR being investigated, ranging from Very Good to Very Poor (Table 1).

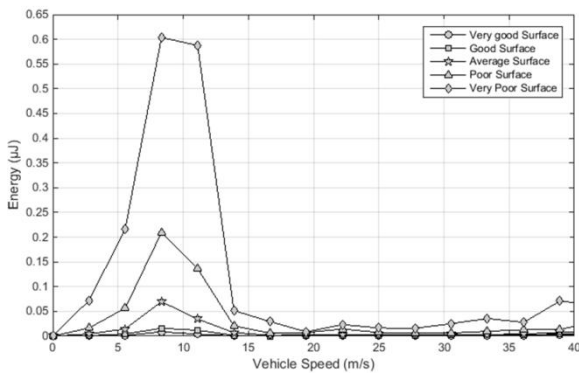


Figure 7.Effect of variation in road surface roughness on energy harvested. A rough road provides higher energy generation.

The effects of RSR on the energy harvesting potential of the bridge are significant, with the Very Poor Surface giving a quantity an order higher than that of a Very Good Surface (Figure 7). A peak of $0.6\mu J$ of energy was obtained for a vehicle passage at $8m/s$ for a Very Poor Surface, with a Poor Surface generating $0.21\mu J$ at a similar speed. It can be seen that Very Good surface conditions correspond to lowest amounts of harvested energy, with a Good surface also generating very low levels of energy. The effect of RSR on the energy harvesting potential is significant, consistent with previous studies on the effects of the RSR on the bridge dynamics. This finding does not indicate that

poorer surfaces are better for monitoring. Better surfaces generate a lower response but are more consistent and thus the question of the best surface for aiding energy harvesting based monitoring is a question of resolution of detection markers against the consistency of such marker values.

4 EFFECTS OF VEHICLE CHARACTERISTICS ON ENERGY HARVESTING

The effect on the energy harvesting potential due to the variance of the vehicle characteristics is investigated next. Three cases are considered in this regard, variation of the vehicle mass, the vehicle stiffness and a combined case of the two. For all cases considered here, the bridge is modelled with centrally located damage of CDR=0.1 and with Road Class E, i.e. Very Poor. The harvester is located at half span.

4.1 Effects of Vehicle Mass on Energy Harvesting

Five vehicles with masses of 0.5, 2.5, 5.0, 7.5, and 10T respectively were considered as per Keane et al. (2012). The results are presented in this sub-section briefly. The comparison with other important operational parameters form a part of the comprehensive study that is presented in this paper. For all cases, the stiffness of the vehicle, as well as other parameters of the system, remain as those of the baseline case. The speed of the vehicle ranges from 0 to $40m/s$. It was found that the 5.0 Tonne class generates substantially more energy than that of the other classes considered, including the heavier 7.5 and 10T classes (Figure 8).

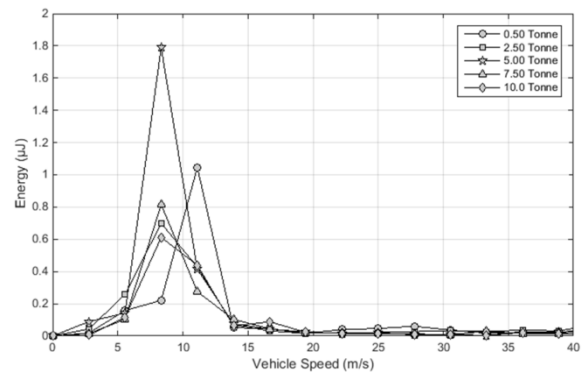


Figure 8.Effect of variation in vehicle mass on energy harvesting potential.

This is due to the increase dynamic response due the heavier vehicle when compared to 0.5 and 2.5T, but not of the order so as to cause the dynamic response of the bridge to be damped, as compared to the 7.5 and 10.0T classes. The peak value obtained was $1.8\mu J$ for the 5.0T vehicle travelling at a speed of $8m/s$. As in previous cases, for all vehicles considered, an optimal vehicle speed bandwidth for energy harvesting ranging from 8 – $12m/s$. The

0.5Tvehicle has a peak at 12m/s and not 8m/s like all other cases considered in this paper thus far. A very high axle load does not necessarily produce higher levels of energy, with the 0.5Tvehicle generating a higher amount of energy, 1.05 μ J, as compared to 7.5Tvehicle, 0.8 μ J, and the 10.0Tvehicle, which in fact provides the lowest peak value of the five weights considered, 0.6 μ J.

4.2 Effects of Vehicle Stiffness on Energy Harvesting

The effect of vehicle stiffness on the output of the energy harvester was next investigated, with five different vehicle stiffness classes considered. Two multiples above and below of the stiffness used previously in this paper, set at $3.65 \times 10^6 N/m$, were considered, resulting in classes with vehicle stiffness of 0.5K, 0.75K, 1.0K, 1.25K, and 1.50K. Again as in previous sections, an optimal bandwidth exists for the energy harvesting output between 8 and 12m/s, with all peak values of the five stiffness classes again being at 8m/s (Figure 9). It was found that with increasing stiffness of the vehicle, the energy harvested increases, ranging from 0.38 μ J for the stiffness class 0.5K up to a peak of 0.9 μ J for class 1.5K. At vehicle speeds outside of the bandwidth, the energy harvesting values are again low. The stiffness of the vehicle was found to influence the energy harvesting potential of the bridge, but less than that of the mass of the vehicle.

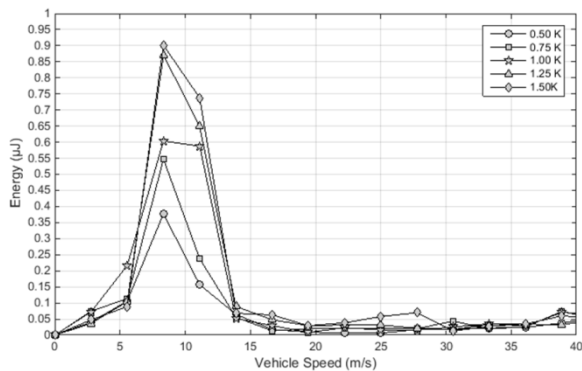


Figure 9.Effect of variation in vehicle mass on energy harvesting potential.

4.3 Combined Effects of Vehicle Mass and Stiffness on Energy Harvesting

The variation of both vehicle mass and stiffness were subsequently investigated to identify the combinations more conducive to the energy harvesting. As such, extreme values are considered with four combinations chosen, with the mass varying from 3,000kg to 40,000kg and the stiffness from $1 \times 10^6 N/m$ to $10 \times 10^6 N/m$ (Table 3), with all other parameters remaining unvaried. It was found that the

best combination was a Heavy Vehicle with a Low Stiffness, which produced an energy of 0.018 μ J at a speed of 12m/s (Figure 10), whilst there is no discernible peak for the Heavy Vehicle with High Stiffness due to lower dynamic effects. For both of these cases, the vehicle speed bandwidth for optimal energy harvesting is larger than previously found. As was noted earlier, the mass is the dominant variable when compared with the stiffness and the Light Vehicle produced very low energy outputs irrespective of the stiffness.

Table 3. Combinations of Vehicle Mass and Stiffness for Energy Harvesting Potential

Condition	Stiffness (N/m)	Mass (kg)
Low Stiffness - Light Vehicle	1×10^6	3,000
Low Stiffness - Heavy Vehicle	1×10^6	40,000
High Stiffness - Light Vehicle	10×10^6	3,000
High Stiffness - Heavy Vehicle	10×10^6	40,000

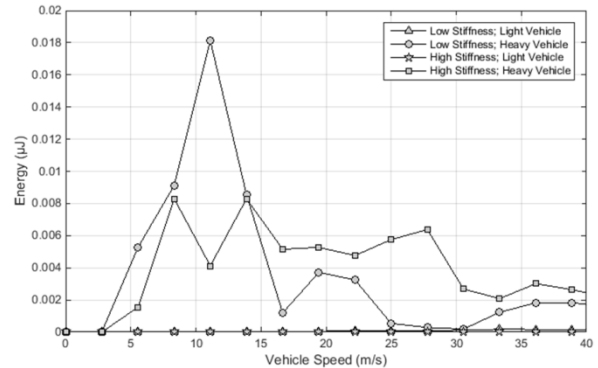


Figure 10.Effect of variation in vehicle mass on energy harvesting potential.

INFLUENCE OF ENERGY HARVESTER WITH VARIABLE NATURAL FREQUENCY ON ENERGY OUTPUT

For a linear energy harvesting device it is necessary to tune the harvester frequency with one of the first few natural frequencies of the bridge. The tuning of the natural frequency of the harvesting device to that of the bridge is investigated in this section. The input to the harvester is the output acceleration and the frequency. The content of the input is dependent on the speed of the vehicle, the natural frequency of the bridge, inertial coupling with the vehicle, bilinear damage and the road surface roughness.

Tuning the harvester to optimal frequencies for vehicular passages would require continuous altering of the harvester's characteristics, which would require energy and negate any benefits or applications of the energy harvester. Energy harvesters with five different natural frequencies are investigated in this regard, with two multiples above and below the natural frequency of the bridge considered. This

results in harvester of $0.50\omega_n$, $0.75\omega_n$, $1.00\omega_n$, $1.25\omega_n$, and finally $1.50\omega_n$. The beam was modelled once again with a centrally located damage of $CDR=0.1$ and with Road Class E, i.e. very poor.

It was found that the energy harvester with a natural frequency tuned to $1.25\omega_n$ produced the largest energy yield when compared to the other four tuning ratios, with a peak of $7.5\mu J$ (Figure 11). The harvester tuning $1.50\omega_n$ produced the second largest energy, $2.4\mu J$, followed by the tuning $1.00\omega_n$. The vehicle speed bandwidth for optimal energy harvesting experiences increased for the harvester $1.25\omega_n$ from between $3m/s$ and $12m/s$, with the peak located at $6m/s$. Again as in previous cases, speeds outside the optimal bandwidth produced relatively small amounts of energy.

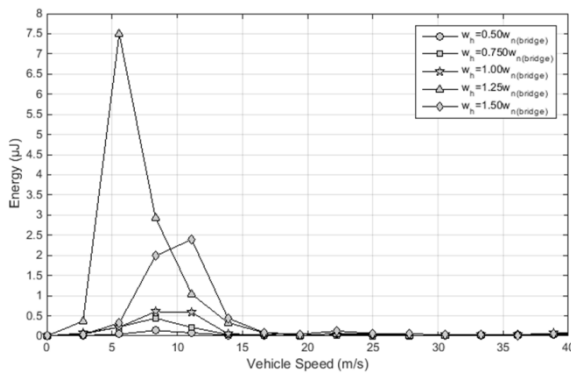


Figure 11. Effect on energy harvesting potential of variation of harvester natural frequency as a function of the natural frequency of the bridge.

6 THEORETICAL AND EXPERIMENTAL ANALYSIS OF ENERGY HARVESTING FROM BRIDGE-VEHICLE INTERACTION

The use of bridge-vehicle interactions as a mechanism for energy harvesting using theoretical simulations has been shown, with the influence of different characteristics determined. The next step is to investigate the experimental validation of energy harvesting devices utilising such interactions and determine the validity of such theoretical simulations. In this regard, the energy harvesting potential from a three dimensional finite element model of train-bridge interaction is now considered. The use of such a model compliments the two dimensional model as used in the preceding sections by illustrating that models of varying degrees of complexity can be utilised when determining the energy harvesting potential from bridge infrastructure. Such a model has previously been utilised to investigate the use of patch based energy harvesters to determine the energy harvesting potential from train-bridge interaction and subsequent SHM applications (Cahill et al., 2014). The use of such a model for energy harvesting using a cantilever

based energy harvester has yet to be studied, and as such, the theoretical energy harvested from the train-bridge interaction is determined and subsequently compared to a computer aided experimental study of the same.

6.1 Modelling of Train-Bridge Interaction using Finite Element Software

To determine the energy harvesting potential from train-bridge interaction, a three dimensional finite element model was created using Strand7 Finite Element Software. The double-track section model was created, with a length of $10.6m$ and width of $10m$ (Figure 12), and two sets of concrete sleepers modelled on the bridge deck at distances of $0.8m$, on which model train tracks were created. The computed natural frequency of the bridge was $12.83Hz$, with the bridge parameters given in Table 4. For modelling of the train passage, loading paths were applied along the length of one of the model tracks on which dynamic point loads were applied to the structure. The individual axle loads of the train are applied at distances and magnitudes as determined by the axle spacing and loading of the train considered. The train considered here is that of a 201Loco, a six axle Irish diesel locomotive hauling seven carriages with four axles each. The axle load of the locomotive and the carriages are $182.5kN$ and $117.7kN$ respectively. The response of the model was determined using a linear transient solver, with the train speed set to $100km/hr$. The acceleration response at the mid-span of the bridge due to this passage was obtained, for subsequent use to determine the energy harvesting potential of a piezoelectric energy harvester, both theoretically and experimentally.

Table 4. Parameters of finite element bridge used for train-bridge interaction simulations

	Symbol	Value	Unit
Bridge			
Length	L	10.6	m
Damping ratio	Z	2.148	%
Youngs Modulus	E	38×10^9	N/m^2
Density	P	2400	Kg/m^3
Second moment of area about the neutral axis	I	33.366	m^4
Height	H	0.8	m
Breadth	B	10.6	m
Cross-Sectional Area	A	4.4	m^2

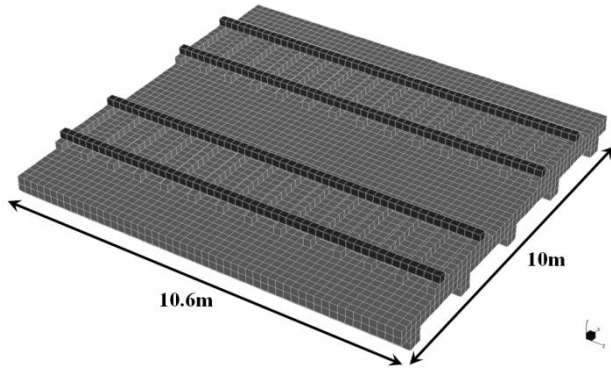


Figure 12. Three dimensional finite element model of dual-track train bridge.

6.2 Fabrication and Setup of Experimental Piezoelectric Energy Harvester

For the experimental analysis of the energy harvesting potential from bridge-vehicle interaction, a cantilever based energy harvester was constructed. A base substrate was constructed using an aluminium beam of width 25mm and thickness 1.25mm , onto which a $52\mu\text{m}$ piezoelectric PolyVinylidene Fluoride (PVDF) harvester of length 50mm and width 20mm was bonded. A tip mass of 0.03kg was added to the end of the beam and the length was arranged so as to match the natural frequency of the harvester with that of the model bridge, with a final length of 158mm being applied. Through an impulse response test and the analysis of the voltage response of the harvester using a fast fourier transform (FFT), the natural frequency of the harvester was experimentally found to be 12.79Hz , agreeing with the natural frequency of the model bridge to a satisfactory degree.

In order to experimentally determine the energy harvester's potential due to the dynamic response of the model bridge due to the train passage, the energy harvester was attached to a permanent magnet shaker (Figure 13) and connected to a load resistor. Through the use of a waveform generator being applied to the shaker unit, the exact response of the bridge can be replicated experimentally as the base excitation to the harvester. In this way, the signature profile of any structure or model may be recreated in a laboratory setting and the energy harvesting potential from the structure determined for any energy harvester. Through the introduction of an accelerometer to the base of the harvester, the experimental output signal can be monitored and compared against the original input signal, thus ensuring complete accuracy. Through the use of the proposed centralised, computer aided experimental procedure, the experimental analysis of the energy harvester can be performed.



Figure 13. Piezoelectric energy harvester attached to shaker unit for experimental validation of energy harvesting potential from train-bridge interactions.

6.3 Experimental Calibration of Piezoelectric Energy Harvester

The calibration of the energy harvester must first be performed to validate the experimental parameters of the energy harvester. This is performed through the application of harmonic loading of varying frequency and constant magnitude as base excitation to the harvester. In this way the theoretical estimates and experimental results can be compared to ensure compliance. Under excitation of $0.5G$ at a range of frequencies, Equations 7 and 8 were used to determine the theoretical voltage output and compared against the experimental analysis of the energy harvester (Figure 14). It was found that a good correlation existed between the two and the parameters of the energy harvester were determined (Table 5). Following this, the theoretical and experimental potential of energy harvesting from train-bridge interaction can be determined.

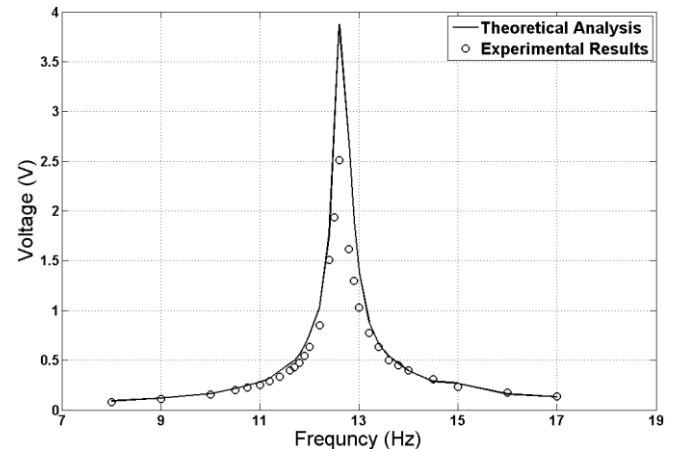


Figure 14. Comparison of theoretical and experimental output of energy harvester for harmonic loading of magnitude 0.5G and varying frequency.

Table 5. Combinations of Vehicle Mass and Stiffness for Energy Harvesting Potential

	Symbol	Value	Unit
Harvester			
Mass	m_h	30	g
Equivalent Viscous Damping Ratio	γ_h	0.04	
Stiffness	k_h	193.741	N/m
Electromechanical Coupling	Θ	1.289	$\mu\text{C/m}$
Capacitance of the Piezoceramic	C_p	1.966	nF
Non-dimensional Time Constant	α	0.158	

6.3 Experimental Validation of Energy Harvesting from Bridge-Vehicle Interaction

The use of the dynamic response of the model bridge due to the train loadings was utilised as the base excitation for the experimental energy harvester, from which the experimental voltage was obtained and compared against the theoretical predictions (Figure 15). Utilising the accelerometer to obtain the experimental output signal, it was found that the acceleration response applied to the harvester was in agreement with the theoretical response of the model bridge (Figure 15(a)). The voltage response from the experimental and theoretical analysis resulted again in comparable response profiles (Figure 15(b)). The root mean squared voltage (V_{rms}) of the theoretical voltage was computed as 0.140V and the experimental voltage was found to be 0.135V. This corresponds to a theoretical energy output of $0.0175\mu\text{J}$ and an experimental energy output of $0.0169\mu\text{J}$.

This experimental analysis illustrates that, through the use of appropriate computer aided experimental setup as proposed here, the performance of an energy harvesters can be validated for bridge-vehicle interactions in a laboratory setting. Such a setup is not confined to bridge structures and can be adopted for any potential civil infrastructure element to determine the energy harvesting potential arising from the application of energy harvesters.

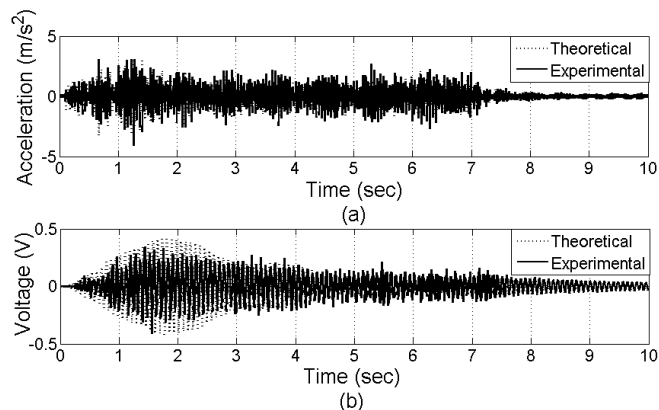


Figure 15. Comparison of theoretical and experimental analysis for (a) Acceleration and (b) Voltage output

7 EFFECTS OF HARVESTER DEPLOYMENT CONSIDERATIONS

7.1 Use of Multiple Harvesters

To understand the effect of using multiple harvesters separated out from the dynamic effects of multiple vehicles, a numerical investigation was carried out using a centrally located crack of $\text{CDR}=0.1$ with Road Class E for the simulated bridge. When considering the spacing for multiple harvesters, size and instrumentation considerations of the harvesters and sufficient spacing for practical purposes must be accounted for. Therefore, a minimum spacing between harvesters is required. Also, as the energy harvesters are dependent on the dynamic response at the location of implementation, the amount of energy harvested at the certain location of the bridge, such as adjacent to the supports, is not sufficient to warrant implementation. Accounting for such limitations, a total of 25 harvesters were considered at a spacing of 300mm centred about the mid-span of the bridge and thus the location of damage, covering 7.5m of span length. The final two harvesters were considered at each of the quarter-spans. The vehicle has the same parameters as that of the baseline case and a single passage is considered. The harvesters were tuned to 1.25 times the natural frequency of the beam based on results obtained in the previous sections. The accumulative peak energy harvested by all 25 harvesting devices produced an output of $60\mu\text{J}$. With increasing numbers of harvesting devices, the increase is not proportional to the number of devices since the harvesting follows the modeshape from which energy is being harvested.

Of note is the power requirement of the accompanying circuitry required for the creation of a SHM system. With advances in low powered electronics, such as the development of wake-up nodes which require μW of power (Magno et al., 2013), the amount of energy harvested in the provided simulations are of sufficient magnitudes to power such a system. Recent advances in intelligent algorithms as also improved the possibility of energy harvesting being used in conjunction with power-hungry sensors (Srbinovski et al., 2016).

7.2 Continuous Harvesting

An ideal condition of continuous energy harvesting over a length is considered next to scrutinize the degree to which a bridge can possibly lend itself towards energy harvesting. Although a closed form expression is not obtained, the problem may be analytically represented from first principles as an undamaged Euler-Bernoulli simply supported beam without surface roughness and traversed by a point load at constant speed, represented by a Dirac Delta function. Considering the first undamaged modeshape, the

ratio of energy harvested (E_h) over the portion of the beam considered centred at the mid-span, L_c , to the energy harvested over the entire length of the bridge (E_{hmax}) can be expressed as

$$\frac{E_h}{E_{hmax}} = \frac{\left(\int_0^\infty \frac{V(t)^2}{R_1} dt \right) \int_{(L-L_c)/2}^{(L+L_c)/2} \sin^2\left(\frac{\pi x}{L}\right) dx}{\left(\int_0^\infty \frac{V(t)^2}{R_1} dt \right) \int_0^L \sin^2\left(\frac{\pi x}{L}\right) dx} = \frac{\frac{L_c}{2} + \frac{\sin\left(\frac{\pi L_c}{L}\right)}{2\pi}}{\frac{L}{2}} = \frac{1}{\pi L} \left(\pi L_c + \sin\left(\frac{\pi L_c}{L}\right) \right) \quad (10)$$

The ratio of L_c/L dominates for larger values of L and the effect of $\left(\sin\left(\frac{\pi L_c}{L}\right) \right) / \pi L$ is only significant for small values of L . Consequently, for most practical cases, the harvested energy ratio will be approximately proportional to the fraction of the length covered about the mid-span. However, for operational purposes, like access, the middle half of the beam may be reasonably considered for effective harvesting.

8 CONCLUSION

Estimates of energy harvested from bridge-vehicle interaction have been obtained in this paper with a view to understand how a number of practical aspects affect the energy harvesting. The potential of energy harvesting for monitoring of bridges and as a possible replacement of low-power, electronic devices is discussed. The modelling approach was validated with detailed finite element simulations and laboratory experiments. The effects of key operational variables involved have been studied and it was found that there exists a relatively narrow vehicle speed bandwidth for which the harvested energy is maximized for a range of road bridges corresponding to the range of typical speeds of traversing of vehicles. Energy harvesting has the potential to distinguish between damaged and undamaged conditions, especially when a local damage is considered. Smeared damages, with more significant change of bending stiffness over a longer zone often exists in bridges under practical conditions and under such circumstances the variation of harvested energy will be more pronounced. Also, for harvesting over a long time, the gradual change in energy harvested can be indicative of the overall bending rigidity of the system.

Road surface unevenness affects the harvested energy to a significant extent. Considering intangible costs to the road user for poor road surfaces, a medium quality road surface is optimum for practical energy yield. A heavier vehicle does not necessarily guarantee a higher yield of energy, nor does a very high stiffness of its tiers and springs. Depending on the bridge and the traversing vehicles, there exist optimum values of vehicular mass and stiffness for which the harvested energy is maximized. The ratio of the natural frequency of the harvesting device to that of the bridge affects the extent of harvested energy. The use of multiple harvesters and multiple vehicles are useful in achieving higher levels of energy but are not proportionate to these numbers. However, higher levels of energy generated have the potential to satisfy the requirements of a range of low powered devices with applications in structural health monitoring. The analysis also emphasizes the potential of using energy harvesting technologies for drive-by assessment of bridges through bridge-vehicle interaction.

ACKNOWLEDGMENTS

The authors wish to thank the Irish Research Council for Science, Engineering and Technology (IRCSET) for providing grant to support this research and CAPACITES/IXEAD society for the practical assistance. The authors also thank Marine Research Energy Ireland (MaREI), grant number 12/RC/2302, a Science Foundation Ireland (SFI) supported project and SFI Advance award 14/ADV/RC3022 and Science Foundation Ireland, International Strategic Cooperation Award (ISCA), Ireland-India ISCA Programme, grant no. 12/ISCA/2493.

REFERENCES

- Abdel-Rohman, M. & Al-Duaij, J. (1996), Dynamic response of hinged-hinged single span bridges with uneven deck. *Computers & Structures*, **59**(2), 291-299.
- Ali, S. F., Adhikari, S., Friswell, M. I. & Narayanan S. (2011a), The analysis of piezomagnetoelastic energy harvesters under broadband random excitations. *Journal of Applied Physics*, **109**(7), 074904.
- Ali, S. F., Friswell, M. I. & Adhikari, S. (2010), Piezoelectric energy harvesting with parametric uncertainty. *Smart Materials and Structures*, **19**(10), 105010(105011-105019).
- Ali, S. F., Friswell, M. I. & Adhikari, S. (2011b), Analysis of energy harvesters for highway bridges. *Journal of Intelligent Material Systems and Structures*, **22**(16), 1929-1938.
- Anderson, A., Ülker-Kaustell, M., Borg, R., Dymen, O., Carolin, A. & Karoumi, R. (2015), Pilot testing of a hydraulic bridge exciter, *MATEC Web Conferences*, **24**, 02001.
- Arms, S., Townsend, C., Churchill, D., Galbreath, J. H. & Mundell, S. W. (2005), Power management for energy

- harvesting wireless sensors, in *SPIE 5763 International Symposium on Smart Structures and Materials 2005, San Diego, California, USA*.
- Beeby, S. P., Tudor, M. J. & White, N. M. (2006), Energy harvesting vibration sources for microsystems applications. *Measurement Science and Technology*, **17**(12), R175-R195.
- Cahill, P., Nuallain, N., Jackson, N., Mathewson, A., Karoumi, R. & Pakrashi, V. (2014), Energy harvesting from train-induced response in bridges. *Journal of Bridge Engineering*, **19**(9), 04014034.
- Challa, V. R., Prasad, M. G. & Fisher, F. T. (2009), A coupled piezoelectric–electromagnetic energy harvesting technique for achieving increased power output through damping matching. *Smart Materials and Structures*, **18**(9), 095029.
- Cho, S. & Spencer, B. F. (2015), Sensor attitude correction of wireless sensor network for acceleration-based monitoring of civil structures. *Computer-Aided Civil and Infrastructure Engineering*, **30**(11), 859-871.
- Elvin, N. G., Lajnef, N. & Elvin, A. A. (2006), Feasibility of structural monitoring with vibration powered sensors. *Smart Materials and Structures*, **15**(4), 977-986.
- Erturk, A. (2011), Piezoelectric energy harvesting for civil infrastructure system applications: Moving loads and surface strain fluctuations. *Journal of Intelligent Material Systems and Structures*, **22**(17), 1959-1973.
- Farinholt, K. M., Miller, N., Sifuentes, W., McDonald, J., Park, G. & Farrar, C. R. (2010), Energy harvesting and wireless energy transmission for embedded SHM sensor nodes. *Structural Health Monitoring*, **9**(3), 269-280.
- Fasl, J., Samaras, V., Reichenbach, M., Helwig, T., Wood, S. L., Potter, D., Lindenberg, R. & Frank, K. (2011), Development of a wireless monitoring system for fracture-critical bridges. *Non-destructive Characterization for Composite Materials, Aerospace Engineering, Civil Infrastructure, and Homeland Security*. San Diego, California, USA, 79831P-79838.
- Fryba, L. (1999), *Vibration of Solids and Structures under Moving Loads*. Thomas Telford Ltd., London.
- Fu, T. S., Ghosh, A., Johnson, E. A. & Krishnamachari, B. (2013), Energy-efficient deployment strategies in structural health monitoring using wireless sensor networks. *Structural Control and Health Monitoring*, **20**(6), 971-986.
- Gillespie, T. D., Karimihias, S. M., Sayers, M. W., Nasim, M. A., Hansen, W., Ehsan, N. & Cebon, D. (1993), Effects of heavy-vehicle characteristics on pavement response and performance. *National Cooperative Highway Research Program*. National Research Council: Transportation Research Board, Washington DC.
- Green, M. F. & Cebon, D. (1994), Dynamic response of highway bridges to heavy vehicle loads: Theory and experimental validation. *Journal of Sound and Vibration*, **170**(1), 51-78.
- Henchi, K., Fafard, M., Talbot, M. & Dhett, G. (1998), An efficient algorithm for dynamic analysis of bridges under moving vehicles using a coupled modal and physical components approach. *Journal of Sound and Vibration*, **212**(4), 663-683.
- Jaksic, V., O' Connor, A. & Pakrashi, V. (2014), Damage detection and calibration from beam–moving oscillator interaction employing surface roughness. *Journal of Sound and Vibration*, **333**(17), 3917-3930.
- Jaksic, V., Pakrashi, V. & O'Connor, A. (2011), Employing surface roughness for bridge-vehicle interaction based damage detection. *ASME 2011 International Mechanical Engineering Congress and Exposition (IMECE 2011): Transportation Systems; Safety Engineering, Risk Analysis and Reliability Methods; Applied Stochastic Optimization, Uncertainty and Probability*. Colorado, pp. 785-793.
- Jaksic, V., Pakrashi, V. & O'Connor, A. (2012), Effect of road quality in structural health monitoring under operational conditions. *Bridge and Concrete Research in Ireland (BCRI)*, Dublin, Ireland.
- Kaur, N. & Bhalla, S. (2014), Combined energy harvesting and structural health monitoring potential of embedded piezo-concrete vibration sensors. *Journal of Energy Engineering*, **141**(4), 4014001.
- Keane, J., O'Sullivan, A., Jaksic, V., Pakrashi, V. & Ali, S. F. (2012), Energy harvesting from beam-moving oscillator interaction in 7th International Workshop on Advanced Smart Materials and Smart Structures Technology ANCRiSST2012, Bangalore, India.
- Kim, S., Pakzad, S., Culler, D. & Demmel, J. (2007), Health monitoring of civil infrastructures using wireless sensor networks. *6th International Symposium on Information Processing in Sensor Networks, 2007*, 254-263.
- Law, S. S. & Zhu, X. Q. (2004), Dynamic behaviour of damaged concrete bridge structures under moving vehicular loads. *Engineering Structures*, **26**(9), 1279-1293.
- Lynch, J. P. (2007), An overview of wireless structural health monitoring for civil structures. *Philosophical Transactions of the Royal Society of London A: Mathematical, Physical and Engineering Sciences*, **365**(1851), 345-372.
- Lynch, J. P. & Loh, K. J. (2006), A summary review of wireless sensors and sensor networks for structural health monitoring. *Shock and Vibration Digest*, **38**(2), 91-130.
- Magno, M., Jackson, N., Mathewson, A., Benini, L. & Popovici, E. (2013), Combination of hybrid energy harvesters with MEMS piezoelectric and nano-Watt radio wake up to extend lifetime of system for wireless sensor nodes. *26th International Conference on Architecture of Computing Systems (ARCS)*, Prague.
- Mann, B. P. & Sims, N. D. (2009), Energy harvesting from the non-linear oscillations of magnetic levitation. *Journal of Sound and Vibration*, **319**(1-2), 515-530.
- Delgado, R. M. & dos Santos, R. C. S. M. (1997), Modelling of railway bridge-vehicle interaction on high speed tracks. *Computers & Structures*, **63**(3), 511-523.

- Narkis, Y. (1994), Identification of crack location in vibrating simply supported beams. *Journal of sound and Vibrations*, **172**(4), 549-558.
- O'Brien, E., Li, Y. & Gonzalez, A. (2006), Bridge roughness index as an indicator of bridge dynamic amplification. *Computers & Structures*, **84**(12), 759-769.
- Pakrashi, V., Kelly, J., & Ghosh, B. (2011), Sustainable prioritisation of bridge rehabilitation comparing road user cost. Transportation Research Board Annual Meeting, 2011.
- Pakrashi, V., O'Connor, A. & Basu, B. (2010a), A bridge-vehicle interaction based experimental investigation of damage evolution. *Structural Health Monitoring*, **9**(4), 285 - 296.
- Pakrashi, V., O'Connor, A. & Basu, B. (2010b), Effect of tuned mass damper on the interaction of a quarter car model with a damaged bridge. *Structure and Infrastructure Engineering*, **6**(4), 409-421.
- Park, J. W., Cho, S., Jung, H. J. & Yun, C. B. (2010), Long-term structural health monitoring system of a cable-stayed bridge based on wireless smart sensor networks and energy harvesting techniques. *5th World Conference on Structural Control and Monitoring (WCSCM) 2010, Tokyo, Japan*.
- Pesterev, A. V. & Bergman, L. A. (1997), Vibration of elastic continuum carrying accelerating oscillator. *ASCE Journal of Engineering Mechanics*, **123**(8), 886-889.
- Renno J.M., Daqaq M.F., & Inman, D.J. (2009) On the optimal energy harvesting from a vibration source, *Journal of Sound and Vibration*, **320** (1-2), 386-405.
- Rice, J., Valdovinos, S., Spencer, B. F. & DeFino, M. (2010), Rapid bridge assessment enabled by wireless smart sensors. *5th World Conference on Structural Control and Monitoring (WCSCM) 2010, Tokyo, Japan*.
- Sazonov, E., Li, H., Curry, D. & Pillay, P. (2009), Self-powered sensors for monitoring of highway bridges. *IEEE Sensors Journal*, **9**(11), 1422-1429.
- Schenk, C. & Bergman, L. (2003), Response of continuous system with stochastically varying surface roughness to moving Load. *ASCE Journal of Engineering Mechanics*, **129**(7), 759-768.
- Shen, H., Qiu, J. & Balsi, M. (2011), Vibration damping as a result of piezoelectric energy harvesting. *Sensors and Actuators A: Physical*, **169**(1), 178-186.
- Sodano, H. A., Park, G., & Inman, D. J. (2004), Estimation of electric charge output for piezoelectric energy harvesting. *Strain*, **40**, 49-58.
- Song, M. K., Noh, H. C. & Choi, C. K. (2003), A new three-dimensional finite element analysis model of high-speed train-bridge interactions. *Engineering Structures*, **25**(13), 1611-1626.
- Srbnovski, B., Magno, M., Edwards Murphy, F., Pakrashi, V., & Popovici E. (2016), An Energy Aware Adaptive Sampling Algorithm for Energy Harvesting WSN with Energy Hungry Sensors. *Sensors*, **16**(4), 448-1-19
- Sundermeyer, J. N. & Weaver, R. L. (1994), On crack identification and characterization in a beam by non-linear vibration analysis. *Journal of Sound and Vibration*, **183**(5), 857-871.
- Torbol, M. (2014), Real time frequency domain decomposition for structural health monitoring using general purpose graphic processing unit. *Computer-Aided Civil and Infrastructure*, **29**(9), 689-702.
- Wu, S. Q. & Law, S. S. (2011), Vehicle axle load identification on bridge deck with irregular road surface profile. *Engineering Structures*, **33**(2), 591-601.
- Yang, Y. B. & Lin, C. W. (2005), Vehicle-bridge interaction dynamics and potential applications. *Journal of Sound and Vibration*, **284**(1-2), 205-226.